A Charging Pricing Strategy of Electric Vehicle Fast Charging Stations for the Voltage Control of Electricity Distribution Networks

Xiaohong Dong[a], Yunfei Mu[a*], Xiandong Xu[b], Hongjie Jia[a*], Jianzhong Wu[b], Xiaodan Yu[a], Yan Qi[c]

[a]*Key Laboratory of Smart Grid of Ministry of Education, Tianjin University, Tianjin 30072, China*

[b]*Institute of Energy, School of Engineering, Cardiff University, Cardiff CF24 3AA, UK*

[c]*Electric Power Research Institute，State Grid Tianjin Electric Power Company，Tianjin 300384，China*

E-mail: [1]dongxiaohong@tju.edu.cn, [2]yunfeimu@tju.edu.cn, [3]xuxiandong87@gmail.com, [4]hjjia@tju.edu.cn, [5]WuJ5@cardiff.ac.uk, [6]yuxd@tju.edu.cn, [7]qiyan_fly@163.com

Author information:

Xiaohong Dong was born in Hebei, China. She is currently pursuing her PhD degree at Tianjin University. Her research interests are electric vehicle charging infrastructure planning and power system stability analysis.

Yunfei Mu (Corresponding author) was born in Hebei, China. He received his PhD degree in the School of Electrical Engineering and Automation, Tianjin University, Tianjin, China, in 2012. He is an Associate Professor of Tianjin University. His main research interests include power system analysis, electric vehicles and smart grids.

Xiandong Xu received his PhD degree in 2015 from Tianjin University, China. He is now a Research Associate at Cardiff University. His research focuses on modelling and flexibility analysis of low-carbon energy systems.

Hongjie Jia was born in Hebei, China. He received his B.S., M.S., and PhD degrees in electrical engineering from Tianjin University, China, in 1996, 1998, and 2001 respectively. He is a Professor of Tianjin University. His research interests include power system stability analysis and control, distribution network planning, renewable energy integration, and smart grids.

Jianzhong Wu received his PhD in 2004 from Tianjin University, China and then worked there from 2004 to 2006. He was a Research Fellow at the University of Manchester from 2006 to 2008. He is currently a Professor in Institute of Energy, Cardiff School of Engineering, U.K. His research activities are focused on energy infrastructure and smart grids.

Xiaodan Yu was born in Liaoning, China. She received her B.S., M.S., and PhD degrees in the electrical engineering from Tianjin University, China, in 1996, 1998, and 2013 respectively. She is an Associate Professor of Tianjin University. Her special fields of interests include power system stability analysis, nonlinear dynamic circuit and the optimal operation of power system.

Detailed address: Room E/627, The building 26, Tianjin University, Weijin Road No.92, Tianjin, 300072, China, Email:yunfeimu@tju.edu.cn, Tel:+86-15822509583

This work was financially funded by the National key research and development program (2017YFB0903300) and the National Natural Science Foundation of China program (Grant No. 51677124 and 51625702).

A Charging Pricing Strategy of Electric Vehicle Fast Charging Stations for the Voltage Control of Electricity Distribution Networks

Xiaohong Dong[a], Yunfei Mu[a*], Xiandong Xu[b], Hongjie Jia[a*], Jianzhong Wu[b], Xiaodan Yu[a], Yan Qi[c]

[a]*Key Laboratory of Smart Grid of Ministry of Education, Tianjin University, Tianjin 30072, China*

[b]*Institute of Energy, School of Engineering, Cardiff University, Cardiff CF24 3AA, UK*

[c]*Electric Power Research Institute, State Grid Tianjin Electric Power Company, Tianjin 300384, China*

E-mail: [1]dongxiaohong@tju.edu.cn, [2]yunfeimu@tju.edu.cn, [3] xuxiandong87@gmail.com, [4]hjjia@tju.edu.cn, [5]WuJ5@cardiff.ac.uk, [6]yuxd@tju.edu.cn, [7]qiyan_fly@163.com

Abstract: With the increasing number of electric vehicles (EVs), the EV fast charging load will significantly affect the voltage quality of electricity distribution networks. On the other hand, EVs have potentials to change the choices of charging locations due to the incentives from the variations of charging prices, which can be considered as a flexible response resource for electricity distribution networks. In this paper, a charging pricing strategy of EV fast charging stations (FCSs) was developed to determine the pricing scheme for the voltage control of electricity distribution networks, which consisted of a simulation model of EV mobility and a double-layer optimization model. Considering the travel characteristics of users, the simulation model of EV mobility was developed to accurately determine the fast charging demand. Taking the total income of FCSs and the users' response to the pricing scheme into account, the double-layer optimization model was developed to optimize the charging pricing scheme and minimize the total voltage magnitude deviation of distribution networks. A test case was used to verify the proposed strategy. The results show that the spatial distribution of EV fast charging loads was reallocated by the proposed charging pricing scheme. It can also be seen that the proposed strategy can make full use of the response capacity from EVs to improve the voltage profiles without decreasing the income of the FCSs.

The short version of the paper was presented at ICAE2017, Aug 21-24, Cardiff, UK. This paper is a substantial extension of the short version of the conference paper.

Keywords: Electric vehicle (EV); Electric vehicle mobility; Charging pricing strategy; Voltage control of electricity distribution networks

1. Introduction

With the growing concerns on the energy depletion and environmental issues around the world, the large-scale adoption of electric vehicles (EVs) is considered as an effective way in decarbonizing the transport sector. In recent years, the EV industry has made considerable progress with the great promotion from governments and automobile enterprises [1]. As the EV supply equipment, the charging infrastructure plays a crucial role in the EVs promotion [2]. With respect to the emergency charging of EVs, the fast charging station (FCS) is becoming the mainstream solution [3]. However, from the view point of electricity distribution networks, the fast charging load will cause the deterioration of voltage quality due to the short charging period and high power demand [4]. Thus, it is necessary to regulate the charging behaviors of EVs so as to improve the voltage quality of electricity distribution networks.

One way to support the operation of distribution networks is the direct control of EV charging load, due to the EVs' flexibility in the charging time and the vehicle-to-grid (V2G) capability [5, 6]. In [7], a hierarchical coordinated charging framework was proposed to generate the charging curve for each aggregator of EVs in order to reduce the peak load of EV charging. In [8], the capacitor, the on-load tap changer and the EV chargers were coordinated to control the voltage of electricity distribution networks. In [9], the on-load tap changers and EVs were collaborated to mitigate the voltage fluctuations caused by generation variations of distributed solar panels. In [10], a high efficient valley-filling strategy was proposed to determine the charging priority of EVs at each time slot. In [11], EV charging loads were separately scheduled by changing the charging times and locations. In [12] , the operation of EV charging behavior was optimized by changing the charging time. In [13], the EV charging scheduling strategy of an aggregator was proposed by regulating the charging power in the charging process. In [14], the charging EV number in a certain period was calculated with the goals of peak-shaving and valley-filling. In [15], a double-layer smart charging strategy was developed. The first layer aims to determine the shortest path for EV users to reach a suitable charger. The second level controls the charging process in order to reduce the charging cost.

The above methods focus on adjusting the battery charging process of EVs. With the development of intelligent transportation systems [16], information and communication technology [17] and fast charging navigation system [18], the price mechanisms were applied to guide the EV charging behaviors.

In [19] and [20], the modeling of the EV driver's response to the charging price was discussed and the EV charging loads were shifted to the valley time period. In [21], the effect of prices on the fast charging behavior of EV users was analyzed. In [22], a proper charging pricing mechanism was designed to guide the EVs' charging behaviors. In [23], the load balancing of FCSs was achieved through a pricing mechanism, considering the quality-of-service targets and the spatial-temporal distribution of EVs. In [24], the fluctuation of renewable energy sources was balanced by adjusting the mobility behavior of EVs with the variations of price signals. The variable electricity prices are calculated based on marginal generation costs. In [25] and [26], it was assumed that the electricity was sold at the wholesale price to the EV users, ignoring FCS interests. And the electricity prices were optimized at the system level considering the operation of the power system and transportation system.

The existing researches have made good contributions to the optimization of EV fast charging load by the price incentives. The FCSs trend to privately-owned facilities [27, 28] and collaborate with distribution networks. Although the charging pricing scheme of FCSs can be applied to improve the voltage quality of distribution networks, the profit of FCSs should be guaranteed when the loads are redistributed through the charging pricing scheme. For this reason, a charging pricing strategy of EV FCSs was proposed to minimize the total voltage magnitude deviation of distribution networks. The charging pricing scheme can be determined to minimize the total voltage magnitude deviation without decreasing the income of FCSs.

2. Framework of the proposed charging pricing strategy

The framework of the proposed charging pricing strategy is shown in Fig. 1, which consists of a simulation model of EV mobility and a double-layer optimization model.

The simulation model of EV mobility: The travel chain method [29], graph theory [30] and the Monte Carlo Simulation (MCS) are used to determine the EV fast charging demand considering the travel characteristics of users. The demand is transferred to the lower layer.

The lower-layer optimization model: According to the fast charging demand supplied by the simulation model and a given charging pricing scheme supplied by the upper layer, the selected FCS of each user is optimized to minimize the corresponding cost. The loads of FCSs and the EV recharging capacity of each user are determined and then transferred to the upper layer.

The upper-layer optimization model: The charging pricing scheme of FCSs is generated and optimized based on the charging loads of FCSs and the EV recharging capacity of each user supplied by the lower layer. The scheme is then transferred to the lower layer.

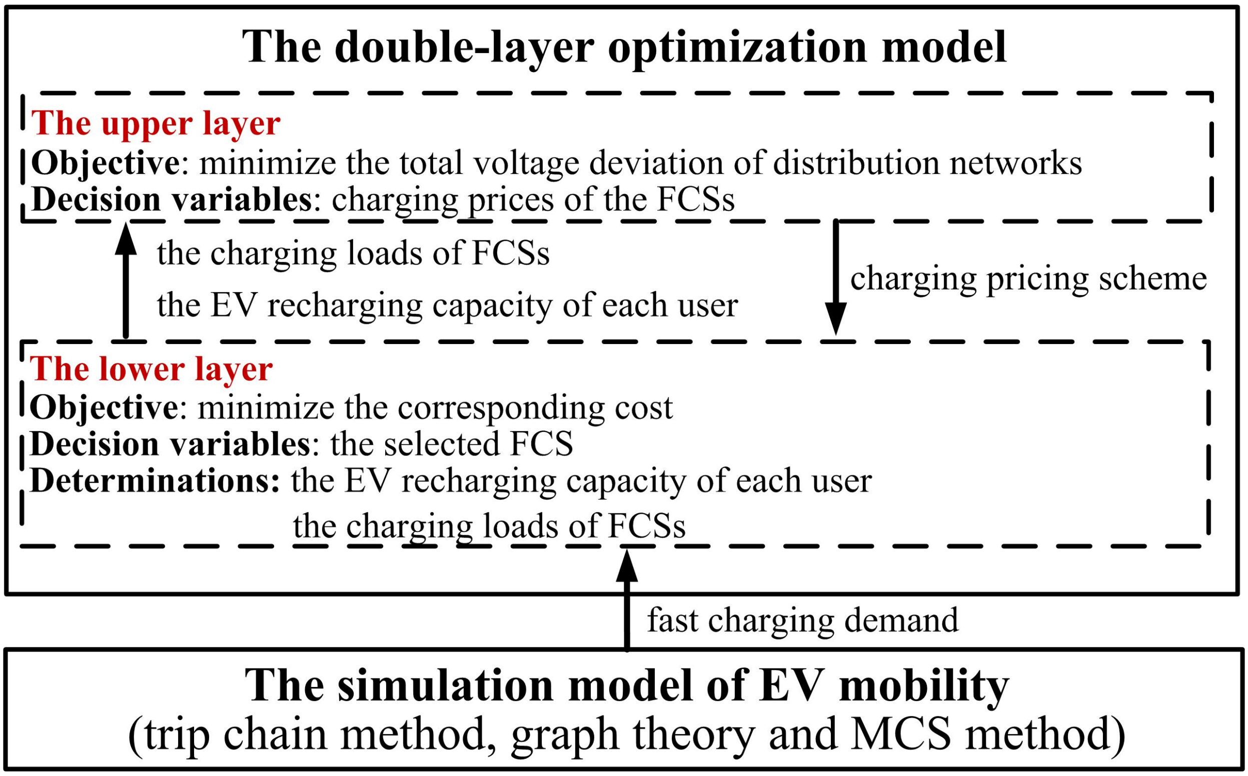

Fig. 1. The framework of the proposed charging pricing strategy

3. The charging pricing strategy

3.1 The simulation model of EV mobility

The EV fast charging demand ***FC*** was predicted by the simulation model of EV mobility, considering the travel characteristics of users and the existing slow charging facilities in the urban area. ***FC*** was then transferred to the lower-layer optimization model.

1) Transportation network model

The extended graph is employed to describe the topology of the transportation network [30]. A graph $\boldsymbol{G}$ is an ordered pair, which consists of a set of vertices $\boldsymbol{V}$ connected by a set of edges $\boldsymbol{E}$. The vertices represent the nodes of the transportation network, while the edges represent the arterial roads and their flow direction. It is assumed that FCSs are built on the arterial roads to avoid the traffic jams. The extended graph includes the virtual vertices representing FCSs and the corresponding edges.

The distance matrix $\boldsymbol{D}$ is used to describe the distances between every two neighbor vertices of the extended graph. $\boldsymbol{D}$ is a $N_v \times N_v$ symmetric matrix and all diagonal elements are zero, where N_v is the total number of vertices in the extended graph and the element $D(v_i, v_j)$ represents the distance from vertex v_i to vertex v_j.

The impedance matrix $\boldsymbol{IM}$ is used to describe the driving time between every two neighbor vertices of the extended graph considering the traffic congestions. $\boldsymbol{IM}$ is determined by $\boldsymbol{D}$ and the average driving speed obtained from the history data of the traffic center. $\boldsymbol{IM}$ is a $Q_1 \times N_v \times N_v$ matrix, where Q_1 is the number of time intervals. And the element $IM(t_1, v_i, v_j)$ of $\boldsymbol{IM}$ represents the driving time from vertex i to j at the time interval t_1.

2) EV mobility model

The EV mobility is closely related with the travel characteristics of users, which is well described by the trip chain [29]. The concept of the trip chain has been widely applied in the travel demand forecast [31][32]. A trip chain is a time-ordered trip sequence which consists of locations and routes of daily trips. This chain can reflect the rules of user's activities in space. In this paper, only the private EVs are considered to forecast their fast charging demand, because other kinds of EVs (such as buses, enterprise owned vehicles, *etc*.) generally have the proprietary charging stations. Also the charging choices of these EVs used for public services are not easy to be changed. The activities of the private EVs are a series of movements and stops describing by the trip chain theory. The trip chain is composed of a spatial chain and a temporal chain.

It is supposed that the battery capacity consumption is linearly dependent on the real driving distance [33]. An energy chain is developed to describe the variations of available battery capacity of EVs with the moments as shown in Fig. 2, based on the trip chain theory. The dotted lines represent travel behaviors and the solid lines indicate parking behaviors. The variables of the spatial chain, the temporal chain and the energy chain for the EV j are listed in Table I.

Table I. The variables of the spatial chain, the temporal chain and the energy chain for the EV j

The variables of the spatial chain		The variables of the temporal chain		The variables of the energy chain	
$s(0)$	The type of the start location of a daily trip chain	ts_0^j	The starting time of the 1th trip	RC_0^j	The initial capacity of the EV battery for the 1th trip
$s(k)$	The type of the k^{th} stop	t_k^j	The driving time of the k^{th} trip	ΔCE_k^j	The power consumption of the k^{th} trip
d_k^j	The driving distance of the k^{th} trip	ta_k^j	The time arriving at the k^{th} stop	$RC_{k,a}^j$	The left capacity of the EV battery arriving at the k^{th} stop
		tr_k^j	The dwell time at the kth stop	ΔC_k^j	The recharging amount of electricity at the k^{th} stop
		ts_k^j	The time leaving the k^{th} stop, namely the starting time of the $(k+1)^{th}$ trip	RC_k^j	The available capacity of the EV battery leaving the k^{th} stop, namely the initial capacity of the $(k+1)^{th}$ trip

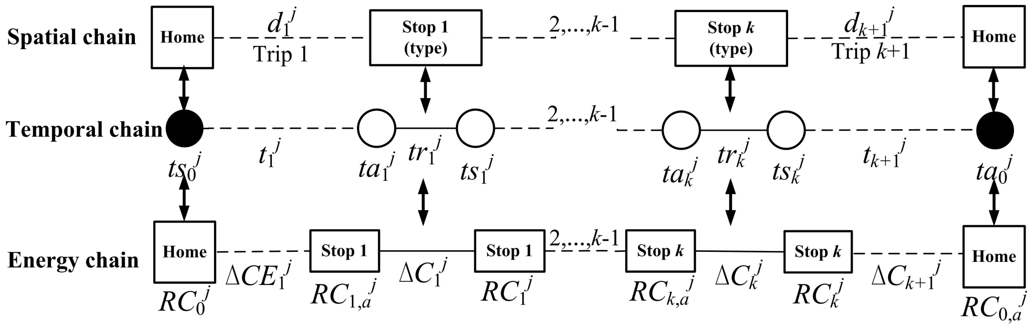

Fig. 2. Schematic diagram of the energy chain

The $\boldsymbol{TY}=\{ty_m|m=1,2,\cdots,Q_2\}$ represents the set of the stop types, where Q_2 is the total number of stop types. It is assumed that the driving distances on the minor roads are ignored and the stops are located at the nodes of the transportation network. The stop type and weight of each node in the transportation network are predefined.

The conditional probability $\boldsymbol{TP}$ is used to describe the transition probability from the stop type ty_v to stop type ty_w, which are determined by the National Household Trip Survey (NHTS) data. $\boldsymbol{TP}$ is a $Q_3 \times Q_2 \times Q_2$ matrix, where Q_3 is the number of time intervals. According to the given time interval t_2, $\boldsymbol{TP}$ is depicted in (1).

$$\boldsymbol{TP}(ty_v,ty_w\,|\,t_2)=\begin{bmatrix} TP(ty_1,ty_1)\,|\,t_2 & \cdots & TP(ty_1,ty_w)\,|\,t_2 & \cdots & TP(ty_1,ty_{Q_2})\,|\,t_2 \\ \vdots & \ddots & \vdots & \ddots & \vdots \\ TP(ty_v,ty_1)\,|\,t_2 & \cdots & TP(ty_v,ty_w)\,|\,t_2 & \cdots & TP(ty_v,ty_{Q_2})\,|\,t_2 \\ \vdots & \ddots & \vdots & \ddots & \vdots \\ TP(ty_{Q_2},ty_1)\,|\,t_2 & \cdots & TP(ty_{Q_2},ty_w)\,|\,t_2 & \cdots & TP(ty_{Q_2},ty_{Q_2})\,|\,t_2 \end{bmatrix} \tag{1}$$

where $TP(ty_v,ty_w|t_2)$ represents the probability that a user transfers from the type ty_v to type ty_w at the time interval t_2. And the sum of probabilities of each row in (1) is equal to 1.

3) Numerical implementation

The following assumptions are adopted in this paper:

1. The EV users, especially the risk-averse ones, reserve a safety margin RC_v to hedge against running out the power capacity.

2. Only fast charging and slow charging with constant power are considered in this paper for the private EV users. It is assumed that all the stops are equipped with enough slow chargers.

3. The EV users will choose the fast charging mode only in emergency.

4. It is assumed that an EV needs at most one fast charging for a day. And the status “stay at home” indicates the travel is finished for the whole day.

The simulation flowchart for the EV fast charging demand is shown in Fig. 3.

Step 1: Set n=1;

Step 2: Set j=1;

Step 3: N_{EV} is the EV number. If $j \leq N_{EV}$, go to Step 5. Otherwise, n=n+1, go to Step 4;

Step 4: N_d is the number of typical days. If $n \leq N_d$, go back to Step 2. Otherwise, save and output the fast charging demand FC;

Step 5: Generate and determine the initial parameters of the EV j; set k=1;

1) Generate ts_0^j based on the probability distributions of ts_0 determined by the NHTS data [34];

2) Generate RC_v^j for the EV j;

3) Determine the battery rated capacity Cap^j of EV j and the power consumption e under the urban dynamometer driving schedule;

4) Determine RC_0^j based on the (2).

$$RC_0^j = SOC_i^j \times Cap^j \tag{2}$$

where SOC_i^j is the initial state of charge for the EV j; it is assumed that the initial state of charge (SOC) varies in the range of [0.8, 0.9], considering the factors such as the battery safety and users’ psychology [35][36].

Step 6: Generate $s(k)$ based on TP, $s(k\text{-}1)$ and $ts_{k\text{-}1}^j$;

Step 7: Determine the stop, d_k^j, t_k^j and tr_k^j;

1) Determine the stop based on $s(k)$ and weights of the transportation network nodes;

2) The travel paths are determined by the modified Floyd algorithm [37] to minimize the driving time of the trip based on IM and $ts_{k\text{-}1}^j$. Thus, d_k^j and t_k^j are determined based on the travel paths and D;

3) Determine tr_k^j based on the probability distribution of tr_k^j according to the NHTS data.

Step 8: Determine ΔCE_k^j based on the (3);

$$\Delta CE_k^j = e \times d_k^j \tag{3}$$

Step 9: If $RC_{k-1}^j<(\Delta CE_k^j+RC_v^j)$, update the fast charging demand *FC*. That is *j,* the stop *k*-1, the stop *k,* RC_{k-1}^j, and RC_v^j are recorded to the matrix ***FC***. And set $j=j+1$ and go back to Step 5. Otherwise, go to Step 10;

Step 10: Determine ta_k^j and ts_k^j based on the (4) and (5).

$$ta_k^j = ts_{k-1}^j + t_{k-1}^j \tag{4}$$

$$ts_k^j = ta_k^j + tr_k^j \tag{5}$$

Step 11: Determine ΔC_k^j, $RC_{k,a}^j$ and RC_k^j based on the (6), (7) and (8).

$$\Delta C_k^j = \begin{cases} \delta_k (RC_0^j - RC_{k,a}^j) & (RC_0^j - RC_{k,a}^j) \le \eta_1 tr_k^j P_{rate}^{slow} \\ \delta_k tr_k^j P_{rate}^{slow} & (RC_0^j - RC_{k,a}^j) > \eta_1 tr_k^j P_{rate}^{slow} \end{cases} \tag{6}$$

$$RC_{k,a}^j = RC_{k-1}^j - \Delta CE_k^j \tag{7}$$

$$RC_k^j = RC_{k,a}^j + \Delta C_k^j \tag{8}$$

where δ_k is the binary variable; δ_k is 1 when the k^{th} stop exists the slow charging facilities and the tr_k^j is larger than the dwell time threshold thr_d. Otherwise δ_k is 0; P_{rate}^{slow} is the rated power of slow charging facilities; η_1 is the slow charging efficiency.

Step 12: If $s(k)$ is "stay at home", set $j=j+1$ and go back to Step 5. Otherwise, set $k=k+1$ and go back to Step 6.

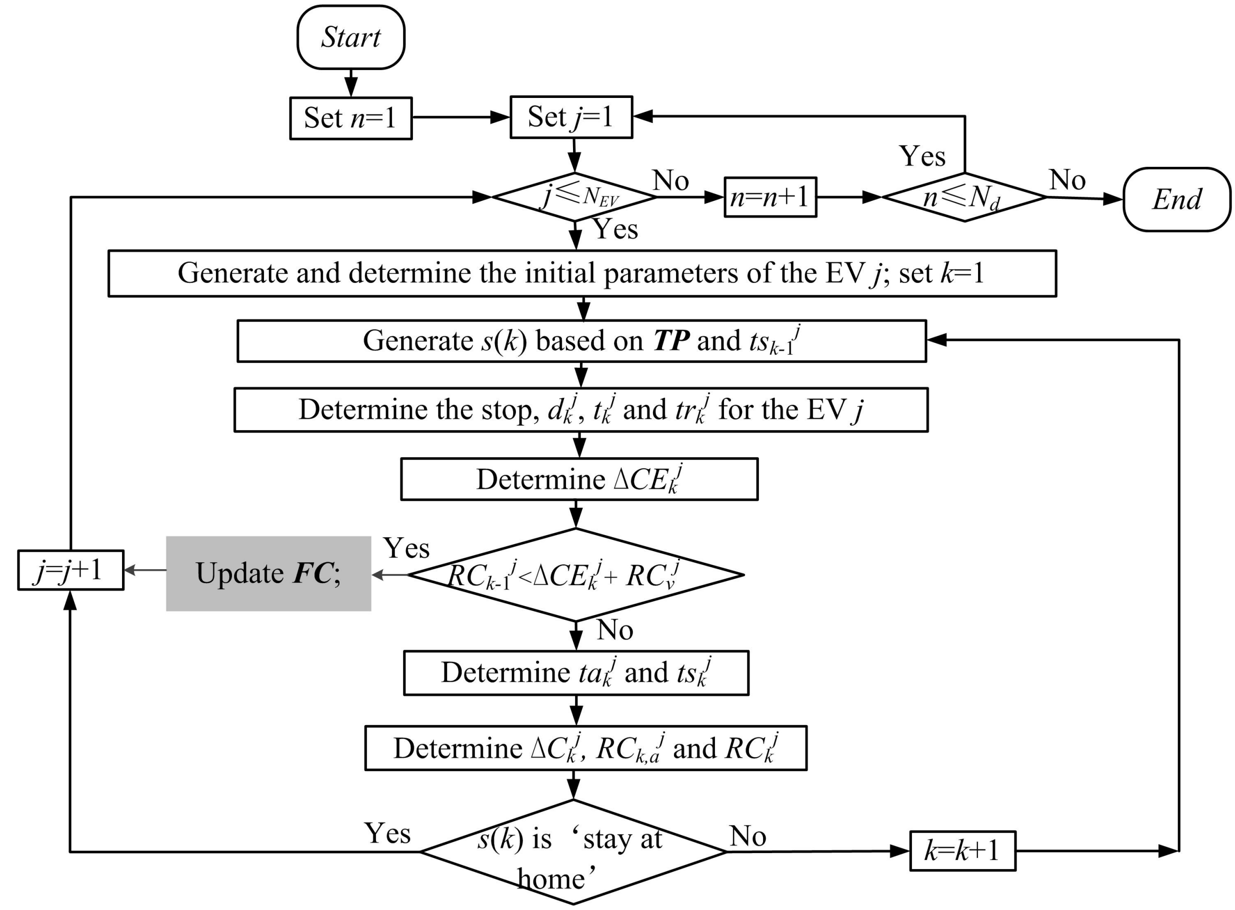

Fig. 3. The simulation flowchart for the EV fast charging demand

3.2 The lower-layer optimization model

The lower-layer optimization model optimizes the selections of users and minimizes the corresponding cost considering the users' response in a given charging pricing scheme from the upper-layer optimization model. The EV recharging capacity for each user and the charging loads of FCSs are determined and then transferred to the upper-layer optimization model.

1) The detour to charge the EV battery

An EV user is assumed to make a detour for a charge when the EV battery runs out of power before reaching the next stop or the destination. For example, when an EV j needs the fast charging from the $(k\text{-}1)^{\text{th}}$ stop to the k^{th} stop, it will make a detour to the FCS i, as shown in Fig. 4. The stop k-1, the stop k, RC_{k-1}^{j}, and RC_{v}^{j} were obtained from ***FC***.

In Fig. 4, $t_{k\text{-}1}^{i}$ is the driving time from the $(k\text{-}1)^{\text{th}}$ stop to the FCS i; t_i^k is the driving time from the FCS i to the k^{th} stop; $d_{k\text{-}1}^{i}$ is the driving distance from the $(k\text{-}1)^{\text{th}}$ stop to the FCS i; d_i^k is the driving distance from the FCS i to the k^{th} stop; $t_{k\text{-}1}^{i}$, t_i^k, $d_{k\text{-}1}^{i}$ and d_i^k are determined by $\boldsymbol{D}$, $\boldsymbol{IM}$ and the modified Floyd algorithm.

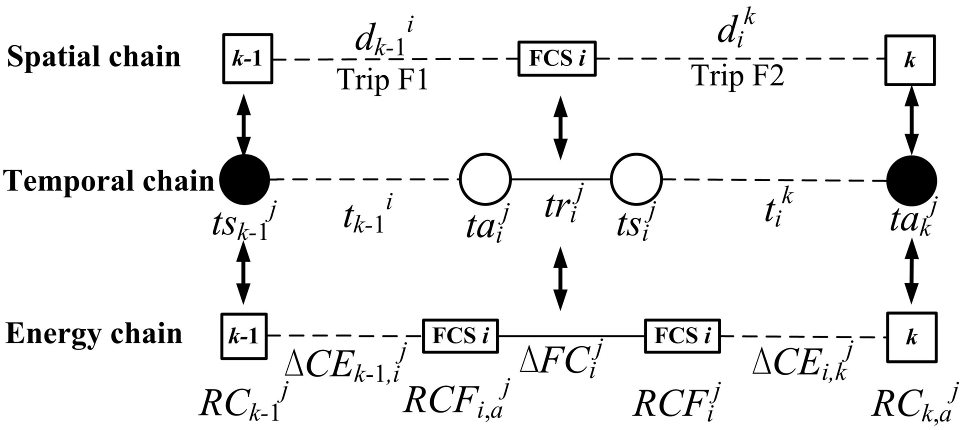

Fig. 4. The chains' diagram of the trip when an EV j needs the fast charging between the $(k\text{-}1)^{\text{th}}$ stop and the k^{th} stop

tr_i^j is the dwell time at the FCS i, as depicted in (9). ta_i^j is the time arriving at the FCS i, as depicted in (10). ts_i^j is the time leaving the FCS i, as depicted in (11). $t_{k\text{-}1}^{k}$ is the total travel time of the trip from the $(k\text{-}1)^{\text{th}}$ stop to the k^{th} stop, as depicted in (12).

$$tr_i^j = tw_i^j + tc_i^j \tag{9}$$

$$ta_i^j = ts_{k-1}^j + t_{k-1}^i \tag{10}$$

$$ts_i^j = ta_i^j + tc_i^j + tw_i^j \tag{11}$$

$$t_{k-1}^k = t_{k-1}^i + t_i^k + tr_i^j \tag{12}$$

For the EV j, tc_i^j is the charging time at the FCS i, as depicted in (13). It is assumed that the available capacity after fast charging is RC_0^j. And ΔFC_i^j is the recharging capacity at the FCS i, as depicted in (14). η_2 is the fast charging efficiency. P_{rate}^{fcs} is the rated power of the fast charger.

$$tc_i^j = \Delta FC_i^j / (\eta_2 \times P_{rate}^{fcs}) \tag{13}$$

$$\Delta FC_i^j = RC_0^j - (RC_{k-1}^j - d_{k-1}^i \times e) \tag{14}$$

2) Determine the waiting time

The activities of the EV j at the FCS are shown in Fig. 5. It is assumed that the EVs are served based on a firstcome first-served rule. The arrival and departure of the EVs at the FCS are shown in Fig. 6 which is taken as an example. Before the time m_1, the accumulated amounts of EV arrival and departure are 4 and 1, respectively. If there are only 2 chargers available at the FCS, the EV j_1 is queuing to wait for charging. At the time l_1, the accumulated amount of EV departure is 3. So no EVs are queuing before the EV j_1 and there is an idle charger at the time l_1. The EV j_1 will start to charge at the time l_1 and its waiting time is l_1-m_1.

Based on the chronological order, the two sets ($\boldsymbol{A}$ and $\boldsymbol{B}$) are used to record the arrival and departure time of the EVs at the FCS, respectively. $size(\boldsymbol{A}(t))$ and $size(\boldsymbol{B}(t))$ are the accumulated amounts of EV arrival and departure at the FCS before the time t. $nev(i,t)$ is the existing EV number at the FCS i at the time t, which is depicted in (15). When $nev(i,ta_i^j)$ is less than the charger number C_i of the FCS i, the waiting time tw_i^j for the EV j at the FCS i is equal to 0. Otherwise, tw_i^j is the minimum time t satisfying the constraint, as depicted in (16).

$$nev(i,t) = Size(\boldsymbol{A}(t)) - Size(\boldsymbol{B}(t)) \tag{15}$$

$$Size(\boldsymbol{B}(ta_i^j + t)) + C_i > Size(\boldsymbol{A}(ta_i^j)) \quad (ta_i^j + t) \in \boldsymbol{B} \tag{16}$$

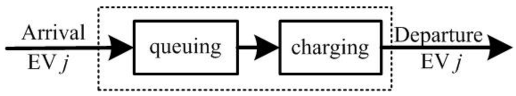

Fig. 5. The activities of the EV j at the FCS

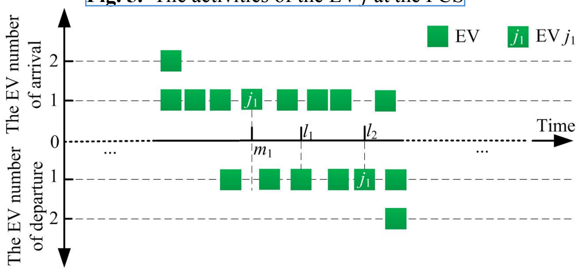

Fig. 6. The arrival and departure of the EVs at the FCS

3) Determine the selections for electric vehicle users

$\boldsymbol{\Omega}_c$ is the set of optional FCSs for the EV j, as depicted in (17), based on the fast charging demand obtained by the simulation model of EV mobility. The EV j can reach the optional FCS i supported by RC_{k-1}^j. And tw_i^j is less than the threshold thr_t at the optional FCS i.

$$\boldsymbol{\Omega}_c = \{i \,|\, \Delta CE_{k-1,i}^j + RC_v^j \le RC_{k-1}^j \;\&\&\; tw_i^j \le thr_t, i \in \boldsymbol{\Omega}\} \tag{17}$$

where $\boldsymbol{\Omega}$ is the set of the FCS serial numbers, namely $\boldsymbol{\Omega}$={1,2,3...,N_{fcs}}; N_{fcs} is the total number of FCSs.

When the EV needs a fast charging, the corresponding user selects the FCS due to different cost priorities. To highlight these priorities, the following three types for the EV j are introduced.

Type I: Selection with the minimum charging cost (fc_i^j), as depicted in (18).

Type II: Selection with the minimum total travel time cost (ft_i^j), as depicted in (19).

Type III: Selection with the minimum total cost (fc_i^j), as depicted in (20).

$$\min fc_i^j = \Delta FC_i^j \times cp_i,\ i \in \boldsymbol{\Omega}_c \tag{18}$$

$$\min ft_i^j = t_k^k \times dc,\ i \in \boldsymbol{\Omega}_c \tag{19}$$

$$\min f_i^j = fc_i^j + ft_i^j,\ i \in \boldsymbol{\Omega}_c \tag{20}$$

where cp_i is the fast charging price of the FCS i obtained by the upper-layer optimization model.

The selection is optimized to minimize the corresponding cost solved by the traversal method in the $\boldsymbol{\Omega}_c$. According to the (14) and (15), ΔFC_i^j and $nev(i,t)$ are determined and transferred to the upper-layer optimization model. $P_{i,t}^{fcs}$ is the average fast charging load of the FCS i at the time interval t as depicted in (21), which is transferred to the upper-layer optimization model.

$$P_{i,t}^{fcs} = \begin{cases} \dfrac{1}{N_d} nev(i,t) \times P_{rate}^{fcs} & nev(i,t) \le C_i \times N_d \\ \dfrac{1}{N_d} C_i \times P_{rate}^{fcs} & nev(i,t) > C_i \times N_d \end{cases} \tag{21}$$

3.3 *The upper-layer optimization model*

The voltage magnitude deviation index developed in [38] was utilized and depicted in (22). $NVD_{n,t}$ represents the voltage magnitude deviation of the node n at the time interval t. $U_{n,t}$ is the voltage magnitude of the node n at the time interval t due to fast charging load. $U_{n,p}$ is the voltage standard value of the node n.

$$NVD_{n,t} = \left\| U_{n,p} \right| - \left| U_{n,t} \right\| \tag{22}$$

It is supposed that FCSs collaborate with distribution networks and the charging prices of FCSs are fixed for a day. The initial charging prices of FCSs are cp_0 and the same. Thus, the fast charging prices of FCSs are optimized to minimize the total voltage magnitude deviation of the distribution networks ($TNVD$), as depicted in

(23). Meanwhile, the total income of the FCSs remains unchanged before and after the optimization as depicted in (24).

$$\min\ TNVD=\sum_{n=1}^{N_D}\sum_{t=1}^{T}NVD_{n,t} \tag{23}$$

$$\sum_{i=1}^{N_{fcs}}cp_i\times\sum_{j\in\boldsymbol{\Omega}(i,cp_i)}\Delta FC_i^j=\sum_{i=1}^{N_{fcs}}cp_0\times\sum_{j\in\boldsymbol{\Omega}(i,cp_0)}\Delta FC_i^j \tag{24}$$

where N_D is the node number in the distribution networks; T is the number of time intervals for a day; $\boldsymbol{\Omega}(i,cp_i)$ and $\boldsymbol{\Omega}(i,cp_0)$ are the sets of the users selecting the FCS i with the charging price cp_i and the cp_0, respectively.

In the model, the following constraints are considered:

1) Upper and lower boundary constraints of the cp_i

To ensure the profit of the FCS, the lower boundary of the charging price should be larger than the electricity price $cp_{\min}$ of the distribution network and the upper boundary of the charging price should be less than the fuel cost converted to the same mileage $cp_{\max}$. The constraints are depicted in (25).

$$cp_{\min}\leq cp_i\leq cp_{\max} \tag{25}$$

2) Voltage constraints

$$U_{n,\min}\leq U_{n,t}\leq U_{n,\max} \tag{26}$$

where $U_{n,\min}$ and $U_{n,\max}$ are the minimum and maximum voltage magnitudes at node n, respectively.

3) Current constraints of lines

$$I_{l,\min}\leq I_{l,t}\leq I_{l,\max}\quad l\in\boldsymbol{\Omega}^L \tag{27}$$

where $I_{l,t}$ is the current of the line l at the time interval t; $I_{l,\min}$ and $I_{l,\max}$ are the minimum and maximum current values of the line l, respectively; $\boldsymbol{\Omega}^L$ is the set of lines.

4) Power flow constraints

$$P_{n,t}=U_{n,t}\sum_{g=1}^{N_D}U_{g,t}(G_{n,g}\cos\theta_{n,g}+B_{n,g}\sin\theta_{n,g}) \tag{28}$$

$$Q_{n,t}{}^{D}=U_{n,t}\sum_{g=1}^{N_D}U_{g,t}(G_{n,g}\sin\theta_{n,g}-B_{n,g}\cos\theta_{n,g}) \tag{29}$$

$$P_{n,t} = P_{n,t}^{D} + \sum_{h \in \boldsymbol{\Omega}_n} P_{h,t}^{fcs} \quad (30)$$

where $P_{n,t}{}^{D}$ and $Q_{n,t}{}^{D}$ are the values of active and reactive power of the node n in the distribution network at the time interval t without fast charging loads from FCSs, respectively; $\boldsymbol{\Omega}_n$ is the set of FCSs connected to the node n of the distribution network.

4. Test case

4.1 Test system and simulation parameters

EVs: four types of private EVs are considered in this case based on the top proportions in the Chinese market on the 2016 as listed in Table II [39]. Based on the NHTS data from US Department of Transportation [34], 6 types of the stops are considered, which are "home", "work" (ty_2), "shopping" (ty_3), "recreation" (ty_4), "pick up somebody" (ty_5) and "meal" (ty_6), respectively. The "home" is further classified into two statuses: "temporary stay at home" (ty_1) and "stay at home" (ty_7) for the stop. ***TP*** is obtained in [40], which is 24×6×7 matrix. ***TP*** at 7:00-8:00 and 17:00-18:00 are shown in Fig. 7. The probability distribution of $ts_0{}^{j}$ and the dwell time for different types of stops can be found in [40].

Transportation network: A real transportation network in the urban core of Hangzhou, China is selected as the test system as shown in Fig. 8, which consists of 116 edges and 42 vertices. The 42 vertices include 31 nodes of the transportation network and 11 FCSs corresponding to 32-41 vertices. In each FCS, there are 8 chargers. The distribution of different stop types is shown in Fig. 8. ***D*** of the 42 vertices is listed in Table III. ***IM*** is obtained from the traffic center [41]. Weights of various stop types for nodes in the transportation network are listed in Table IV.

Electricity distribution network: In China, most FCSs are connected to 10-kV feeder [42]. Each FCS is taken as a centralized load of the 10-kV distribution network. The structures of four 10-kV distribution networks are configured based on the IEEE 33 standard distribution network [43] as shown in Fig. 9. The peak load of each node in the distribution networks is listed in Table V. The load profile is obtained from [44].

Other simulation parameters are listed in Table VI.

Table II The main EVs in the Chinese market [45]

EV Manufacturer	EV type	Proportion	The rated capacity of the battery (kWh)	*e* (kWh/km)
BYD	E6	12.17%	57	0.14
BAIC BJEV	EV160	11.11%	25.6	0.13
GEELY NEW ENERGY	EV 300	10.15%	45.3	0.15
ZOTYE AUTO	CLOUD100S	9.70%	18	0.12

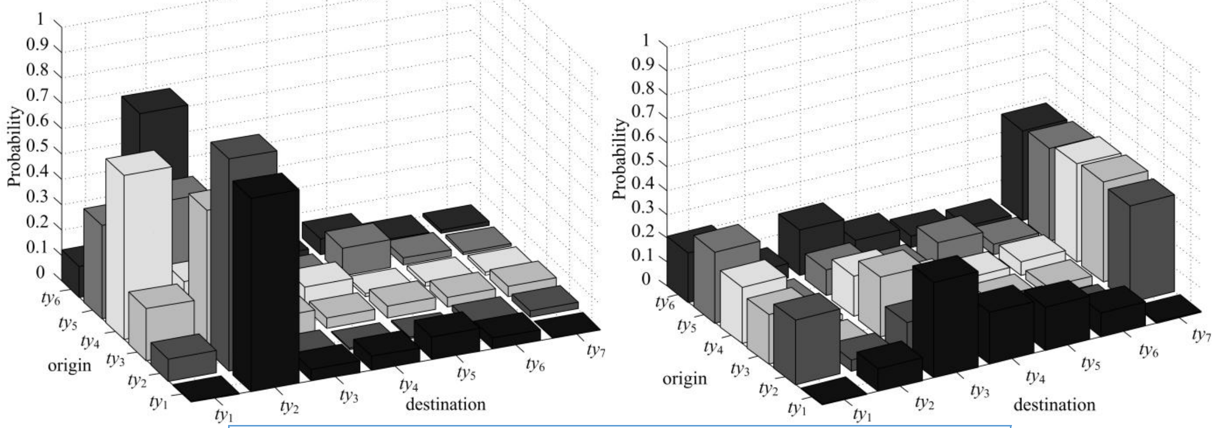

(a) at 7:00-8:00 (b) at 17:00-18:00

Fig. 7. ***TP*** of the stops

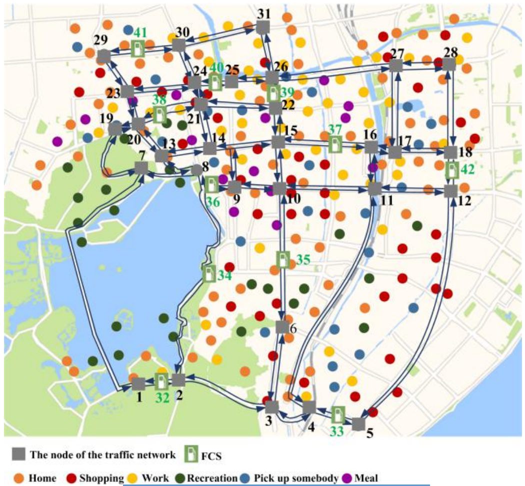

Fig. 8. The transportation network

Table III The distance of neighbor vertices

vi	*vj*	*d*(*vi*, *vj*)	*vi*	*vj*	*d*(*vi*, *vj*)	*vi*	*vj*	*d*(*vi*, *vj*)	*vi*	*vj*	*d*(*vi*, *vj*)	*vi*	*vj*	*d*(*vi*, *vj*)
3	2	10 km	14	13	6 km	23	20	2 km	32	1	2 km	38	20	1 km
4	3	4 km	15	10	2 km	24	21	2 km	32	2	0.5 km	38	21	5 km
6	3	4 km	15	14	4 km	24	23	6 km	33	4	1 km	39	22	1 km
7	1	10 km	16	11	2 km	26	25	1 km	33	5	3 km	39	26	1 km
8	7	2.5 km	17	16	2 km	27	17	4 km	34	2	6 km	40	24	2 km
10	9	4 km	18	17	2 km	27	26	6 km	34	8	4 km	40	25	1 km
11	4	10 km	19	7	4 km	28	18	4 km	35	6	3 km	41	29	3 km
11	10	4 km	20	13	2 km	28	27	2 km	35	10	3 km	41	30	3 km
12	5	10 km	20	19	2.5 km	29	23	2 km	36	8	4 km	42	12	1 km
12	11	4 km	21	14	2 km	30	24	2 km	36	9	2 km	42	18	1 km
13	8	2 km	22	15	2 km	31	26	2 km	37	15	1 km			
14	9	2 km	22	21	4 km	31	30	4 km	37	16	3 km			

Table IV Weights for each node in the transportation network

No.	ty_1	ty_2	ty_3	ty_4	ty_5	ty_6	No.	ty_1	ty_2	ty_3	ty_4	ty_5	ty_6
1	0.06	0.00	0.00	0.18	0.00	0.00	17	0.02	0.00	0.09	0.00	0.09	0.09
2	0.02	0.03	0.00	0.18	0.00	0.00	18	0.07	0.03	0.09	0.00	0.00	0.09
3	0.03	0.03	0.04	0.00	0.00	0.04	19	0.05	0.04	0.05	0.05	0.00	0.05
4	0.00	0.07	0.04	0.04	0.09	0.04	20	0.05	0.03	0.00	0.00	0.00	0.00
5	0.00	0.00	0.04	0.00	0.00	0.04	21	0.00	0.00	0.05	0.00	0.00	0.05
6	0.02	0.00	0.00	0.18	0.00	0.00	22	0.05	0.10	0.00	0.00	0.23	0.00
7	0.03	0.00	0.00	0.18	0.00	0.00	23	0.05	0.03	0.05	0.00	0.00	0.05
8	0.04	0.07	0.05	0.09	0.00	0.05	24	0.05	0.03	0.05	0.00	0.00	0.05
9	0.05	0.00	0.04	0.00	0.00	0.04	25	0.00	0.07	0.05	0.00	0.00	0.05
10	0.02	0.07	0.04	0.00	0.18	0.04	26	0.04	0.07	0.00	0.00	0.00	0.00
11	0.05	0.06	0.00	0.00	0.00	0.00	27	0.03	0.04	0.09	0.00	0.00	0.09
12	0.02	0.00	0.07	0.00	0.00	0.07	28	0.05	0.06	0.05	0.00	0.00	0.05
13	0.08	0.01	0.00	0.09	0.00	0.00	29	0.04	0.00	0.00	0.00	0.14	0.00
14	0.07	0.03	0.11	0.00	0.05	0.11	30	0.00	0.08	0.00	0.00	0.23	0.00
15	0.01	0.04	0.00	0.00	0.00	0.00	31	0.01	0.00	0.00	0.00	0.00	0.00
16	0.05	0.03	0.00	0.00	0.00	0.00							

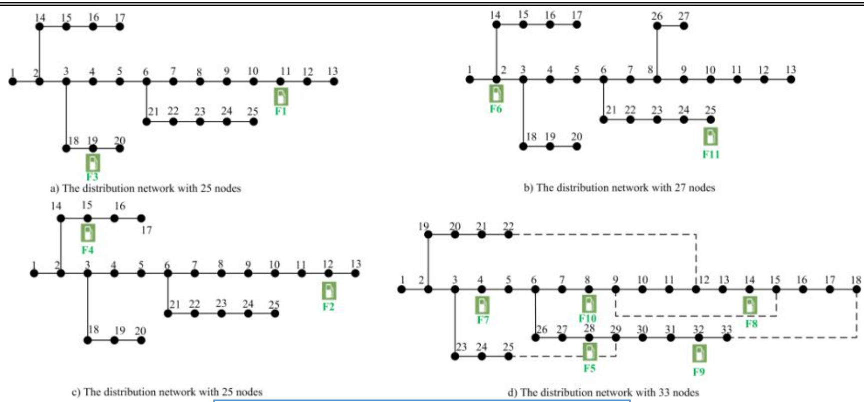

Fig. 9. The corresponding distribution networks

Table V The peak load for each node in the corresponding distribution networks

The distribution network with 25 nodes (MVA)						The distribution network with 27 nodes (MVA)					
No.	Peak load	No.	Peak load	No.	Peak load	No.	Peak load	No.	Peak load	No.	Peak load
1	0	10	0.06+j0.02	19	0.42+j0.2	1	0	10	0.06+j0.02	19	0.42+j0.2
2	0.1+j0.6	11	0.045+j0.03	20	0.42+j0.2	2	0.1+j0.6	11	0.045+j0.03	20	0.42+j0.2
3	0.09+j0.04	12	0.06+j0.035	21	0.06+j0.025	3	0.09+j0.04	12	0.06+j0.035	21	0.06+j0.025
4	0.12+j0.08	13	0.06+j0.01	22	0.06+j0.025	4	0.12+j0.08	13	0.06+j0.01	22	0.06+j0.025
5	0.06+j0.03	14	0.09+j0.04	23	0.06+j0.02	5	0.06+j0.03	14	0.09+j0.04	23	0.06+j0.02
6	0.06+j0.02	15	0.09+j0.04	24	0.12+j0.07	6	0.06+j0.02	15	0.09+j0.04	24	0.12+j0.07
7	0.06+j0.035	16	0.09+j0.04	25	0.2+j0.6	7	0.06+j0.035	16	0.09+j0.04	25	0.2+j0.6
8	0.06+j0.02	17	0.09+j0.04			8	0.06+j0.02	17	0.09+j0.04	26	0.09+j0.04
9	0.2+j0.1	18	0.09+j0.05			9	0.2+j0.1	18	0.09+j0.05	27	0.12+j0.8

Table VI The other simulation parameters

The parameter	Value	Unit	The parameter	Value	Unit
Q_1	96	-	dc	17 [47]	RMB/h
Q_3	24	-	$U_{d,\min}$	0.9	-
RC_v^j	0,1,2	kWh	$cp_{\min}$	1.08	RMB/kWh
thr_d	120	min	$cp_{\max}$	3.3	RMB/kWh
η_1	90	%	cp_0	1.6 [45]	RMB/kWh
P_{rate}^{slow}	3.3	kW	N_d	100	day
η_2	99 [48]	%	N_{EV}	30000	-
P_{rate}^{fcs}	120	kW	T	96	-
thr_t	20	min	$U_{n,p}$	1	-

4.2 The results and analysis

1) Optimal results and analysis

The EV users of Type I, Type II and Type III account for 40%, 30% and 30%, respectively. The optimal charging pricing scheme of the FCSs is shown in Fig. 10. The results provide a pricing scheme for the FCSs to remain the FCS total income while the voltage profiles of the distribution networks are improved. Compared with the cp_0 pricing scheme, the fast charging prices of the FCS 4, 7 and 10 are lower, while the fast charging prices of the remaining FCSs are higher.

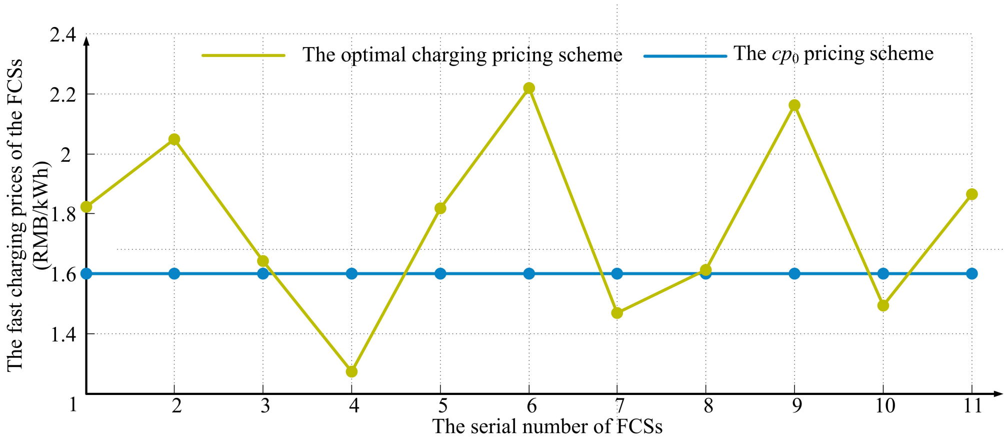

Fig. 10. The optimal charging pricing scheme of the FCSs

The load difference between the optimal charging pricing scheme and the cp_0 pricing scheme is shown in Fig. 11. The fast charging loads are reallocated among the spatial adjacent FCSs in response to the pricing scheme. Because the FCS 6 price is larger than the FCS 4 price, the FCS 6 load is partially transferred to the FCS 4. Compared with the corresponding load under the cp_0 scheme, the FCS 6 load under the optimal pricing scheme is decreasing, while the FCS 4 load is increasing. That is, the fast charging load at the node 2 of the distribution network b is partially transferred to the node 15 of the distribution network c. Similarly, because the FCS 11 price is larger than the prices of the FCS 4 and 8, the FCS 11 load is partially transferred to the FCS 4 and 8. Thus, the FCS 11 load under the optimal pricing scheme is decreasing compared with the load under the cp_0 scheme. Because the loads are partially transferred to other nodes of other distribution networks, the voltage profiles of distribution network b under the optimal pricing scheme are improved as shown in Fig. 12.

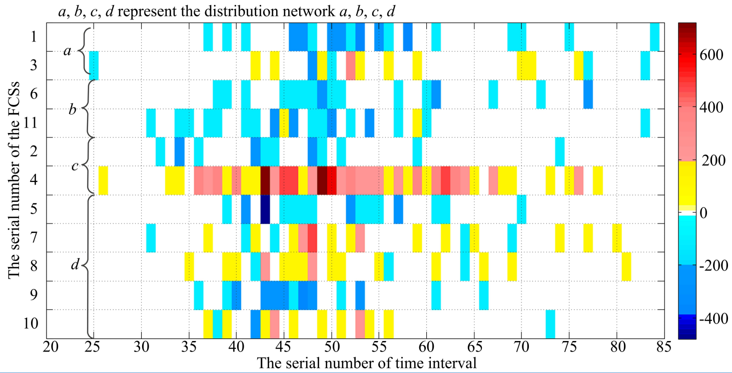

Fig. 11. The FCS load difference between the optimal pricing scheme and the cp_0 scheme

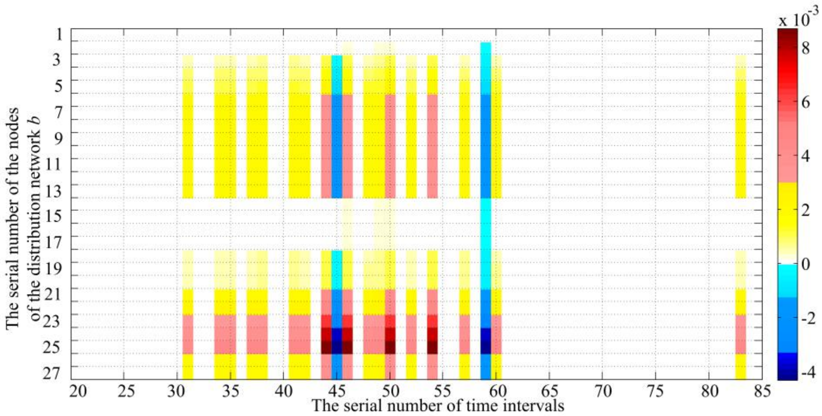

Fig. 12. The voltage magnitude difference between the optimal pricing scheme and the cp_0 scheme

2) Comparison and analysis

In order to verify the effectiveness of the proposed strategy in this paper, three scenarios are considered for N_{EV} EVs and the corresponding results are compared and analyzed.

Scenario I: The EV users of Type I, Type II and Type III account for 20%, 50% and 30%, respectively.

Scenario II: The EV users of Type I, Type II and Type III account for 40%, 30% and 30%, respectively.

Scenario III: The EV users of Type I, Type II and Type III account for 50%, 20% and 30%, respectively.

The optimal pricing schemes under different scenarios are shown in Fig. 13. Compared with the total voltage magnitude deviation $TNVD_0$ of the distribution networks with the cp_0 scheme, $TNVD$ is shown in Fig. 14 under different scenarios. The total voltage magnitude deviations for different distribution networks under different scenarios are listed in Table VII. The differences between $TNVD_0$ and $TNVD$ under these scenarios are also listed in Table VII.

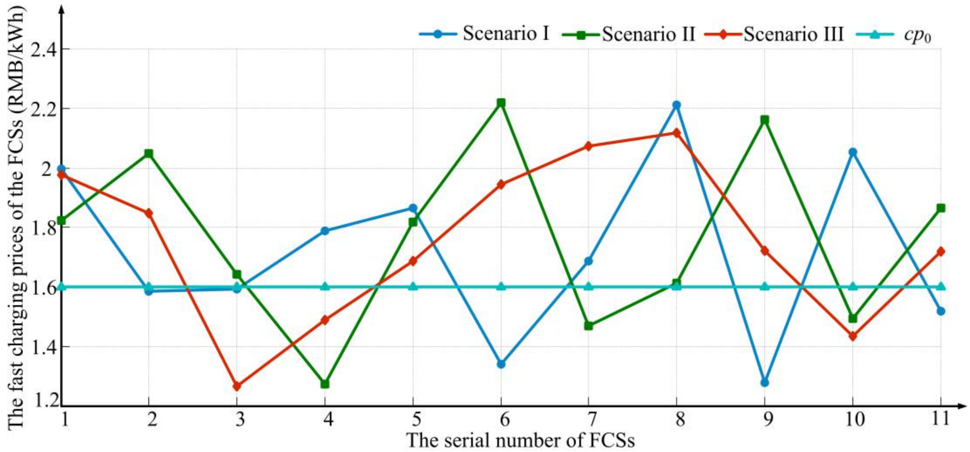

Fig. 13. The optimal charging pricing schemes compared with the cp_0 pricing scheme under different scenarios

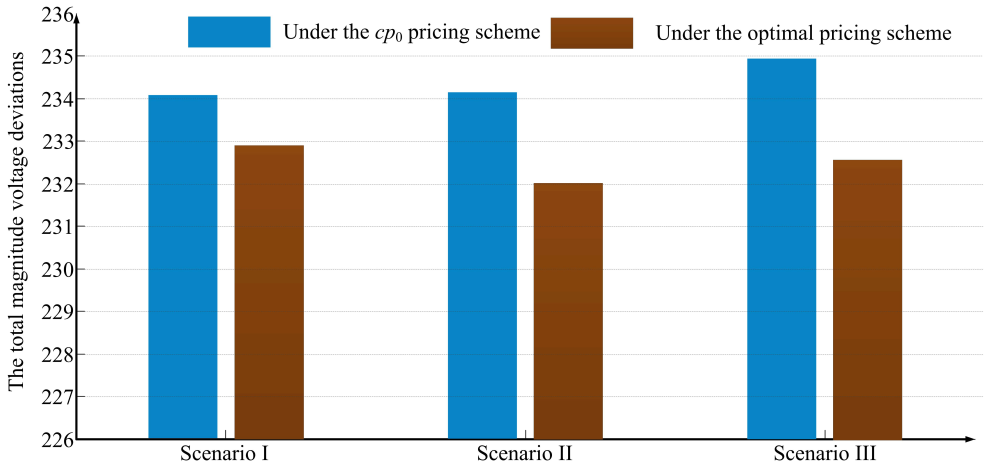

Fig. 14. *TNVD* compared with $TNVD_0$ under different scenarios

Table VII The total voltage magnitude deviations for different distribution networks under different scenarios

Scenario	The voltage magnitude deviations	Distribution network *a*	Distribution network *b*	Distribution network *c*	Distribution network *d*	The difference between $TNVD_0$ and *TNVD*
I	Under the optimal pricing scheme	50.2684	62.8003	49.9785	69.8459	1.1951
	Under the cp_0 scheme	50.7840	63.4273	50.2758	69.6011	
II	Under the optimal pricing scheme	49.9201	62.792	50.4169	68.8859	2.1247
	Under the cp_0 scheme	50.977	63.5656	50.4763	69.1208	
III	Under the optimal pricing scheme	50.9933	63.2646	49.9685	68.3356	2.3737
	Under the cp_0 scheme	51.4274	63.411	50.6303	69.4671	

TD and TD_0 are the sums of $d_{k\text{-}1}{}^{j}$ for all the EVs before and after the optimization, respectively. *TD* and TD_0 under different scenarios are shown in Fig. 15. Because some EV users will select relatively far FCS due to the optimal pricing scheme, *TD* is larger than TD_0 under each scenario. Thus, EV users' convenience for the fast charging is reduced, which indicates the voltage profiles of the distribution networks are improved at the expense of the EV users' convenience on the whole.

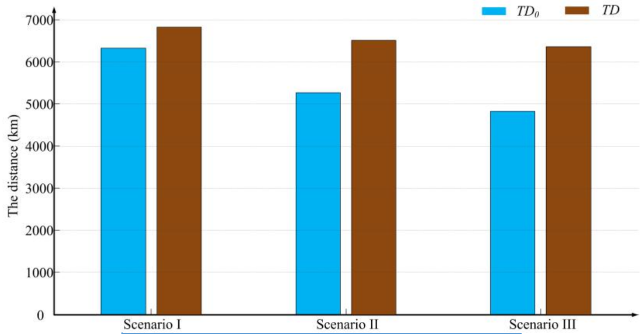

Fig. 15. TD_0 and TD under different scenarios

The difference of the sum of $d_{k\text{-}1}^{j}$ before and after the optimization for different users is listed in Table VIII. Type I and Type III users respond to the prices, so the sum of $d_{k\text{-}1}^{j}$ for these users under each scenario is different before and after the optimization. Type II users do not respond to the prices, so TD_2 is equal to TD_{20}. The distribution of EV fast charging loads is changed and the voltage profiles of distribution networks are improved. More users respond to the optimal pricing scheme and the difference between $TNVD$ and $TNVD_0$ is larger, as shown in Table VII.

Table VIII The difference of the sum of $d_{k\text{-}1}^{j}$ before and after the optimization for different users

	The difference between TD_1 and TD_{10}* (km)	The difference between TD_2 and TD_{20}* (km)	The difference between TD_3 and TD_{30}* (km)
Scenario I	688.5	0	-185.5
Scenario II	1399.5	0	-160
Scenario III	1764	0	-224

*TD_1, TD_2 *and* TD_3 are the sums of $d_{k\text{-}1}^{j}$ for Type I, Type II and Type III users under the optimal pricing scheme, respectively. TD_{10}, TD_{20} and TD_{30} are the sums of $d_{k\text{-}1}^{j}$ for Type I, Type II and Type II users under the cp_0 scheme, respectively.

The cost difference before and after the optimization for different users is listed in Table IX. If the difference is positive, the corresponding cost is increased after the optimization. FC_1 and F_3 are decreasing under Scenario I and II, and FT_2 is not changed after the price optimization. However, F_3 is increased after the optimization under Scenario III. It indicates that the optimal pricing scheme will increase the total cost of Type III users with the proportion increase of Type I users, to some extent.

Table IX The cost difference before and after the optimization for different users

	The difference between FC_1 and FC_{10}* (RMB)	The difference between FT_2 and FT_{20}* (RMB)	The difference between F_3 and F_{30}* (RMB)
Scenario I	-232.37	0	-190.66
Scenario II	-231.17	0	-65.22
Scenario III	-392.26	0	175.64

*FC_1 and FC_{10} are the sums of the charging cost for Type I users under the optimal pricing scheme and cp_0 scheme, respectively. FT_2 and FT_{20} are the sums of the total travel time cost for Type II users under the optimal pricing scheme and cp_0 scheme, respectively. F_3 and F_{30} are the sums of the total cost for Type III uses under the optimal pricing scheme and cp_0 scheme, respectively.

3) The sensitivity analysis of the EV number

The sensitivity of the EV number on the *TNVD*/$TNVD_0$ is analyzed and shown in Fig. 16. *TNVD* and $TNVD_0$ grow with the EV number increasing from 10000 to 50000 at a fixed step. However, the difference between $TNVD_0$ and *TNVD* keeps increasing. This is because more EVs will respond to the optimal pricing scheme as the EV number increases.

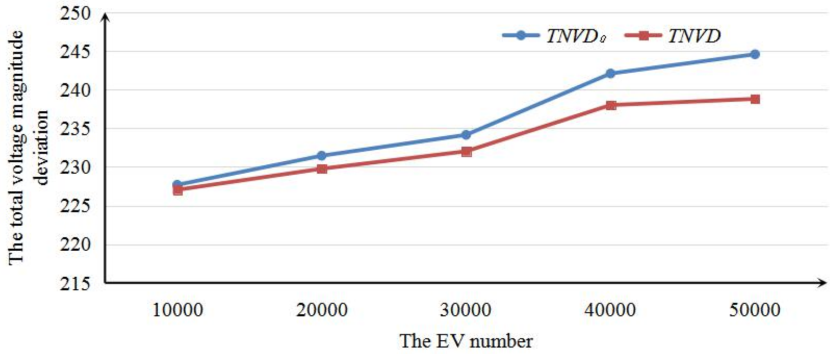

Fig. 16. $TNVD_0$ and *TNVD* under different EV numbers

5. Conclusion and future work

This paper develops a charging pricing strategy of EV FCSs for the voltage control of electricity distribution networks. Considering the travel characteristics of EV users, the fast charging demand is determined using an energy chain. Through the coordination between the upper and lower layers, the fast charging prices are optimized to minimize the total voltage magnitude deviation of distribution networks without decreasing the total income of the FCSs. A real urban transportation network with 11 FCSs is used to validate the proposed strategy.

The results show that the voltage profiles of the test system can be significantly improved due to the reallocated fast charging load by the proposed strategy. This is because the users respond to the optimal charging pricing scheme. The strategy is to fully explore the characteristics of different type EV users, and guide these users to participate in the voltage control of distribution networks. Future research will enhance the EV users' willingness to participate in the voltage control of distribution networks. The game theory will be also introduced to coordinate the benefits of distribution networks, FCSs and EV users.

Acknowledgements

This work was financially funded by the National key research and development program (2017YFB0903300) and the National Natural Science Foundation of China program (Grant No. 51677124 and 51625702).

Reference

[1] International Energy Agency, Global EV Outlook 2017, [Online]. Available: http://www.iea.org/Global EV Outlook 2017.

[2] Madina, C.; Zamora, I.; Zabala, E. Methodology for assessing electric vehicle charging infrastructure business models. Energy Policy 2016, 89, 284-293.

[3] Serradilla, J.; Wardle, J.; Blythe, P.; Gibbon, J. An evidence-based approach for investment in rapid-charging infrastructure. Energy Policy 2017, 106, 514-524.

[4] Rubino L, Capasso C, Veneri O. Review on plug-in electric vehicle charging architectures integrated with distributed energy sources for sustainable mobility. Applied Energy, 2017, 207.

[5] Veneri Ottorino, Technologies and Applications for Smart Charging of Electric and Plug-in Hybrid Vehicles, Springer, 2017.

[6] K. N. Kumar, B. Sivaneasan, P. H. Cheah, et al, “V2G capacity estimation using dynamic EV scheduling,” IEEE Trans. Smart Grid, vol. 5, no. 2, pp. 1051-1060, Mar. 2014.

[7] Xu Z, Hu Z, Song Y, et al. Coordination of PEVs charging across multiple aggregators. Applied Energy, 2014, 136(C):582-589.

[8] Wang M, Wang T, Mu Y, et al. A volt-var optimal control for power system integrated with wind farms considering the available reactive power from EV chargers, Power and Energy Society General Meeting. IEEE, 2016.

[9] Cheng L, Chang Y, Huang R. Mitigating Voltage Problem in Distribution System with Distributed Solar Generation Using Electric Vehicles. IEEE Trans. on Sustainable Energy, 2017, 6(4):1475-1484.

[10] Jian L, Zheng Y, Shao Z. High efficient valley-filling strategy for centralized coordinated charging of large-scale electric vehicles. Applied Energy, 2017, 186:46-55.

[11] Sun S, Yang Q, Yan W. Optimal temporal-spatial PEV charging scheduling in active power distribution networks. Protection & Control of Modern Power Systems, 2017, 2(1):34.

[12] Cheng Y, Zhang C. Configuration and operation combined optimization for EV battery swapping station considering PV consumption bundling. Protection & Control of Modern Power Systems, 2017, 2(1):26.

[13] Han, J.; Park, J.; Lee, K. Optimal scheduling for electric vehicle charging under variable maximum charging power. Energies 2017, 10, 933.

[14] Masoum, A.S.; Deilami, S.; Moses, P.S.; Masoum, M.A.S.; Abu-Siada, A. Smart load management of plug-in electric vehicles in distribution and residential networks with charging stations for peak shaving and loss minimization considering voltage regulation. IET Gener. Transm. Distrib. 2011, 5, 877-888.

[15] Yagcitekin B, Uzunoglu M. A double-layer smart charging strategy of electric vehicles taking routing and charge scheduling into account. Applied Energy, 2016, 167:407-419.

[16] Tulpule P, Marano V, Rizzoni G, et al. A Statistical Approach to Assess the Impact of Road Events on PHEV Performance using Real World Data, SAE 2011 World Congress & Exhibition, 2011.

[17] Cheng X, Hu X, Yang L, et al. Electrified Vehicles and the Smart Grid: The ITS Perspective. IEEE Transactions on Intelligent Transportation Systems, 2014, 15(4):1388-1404.

[18] Guo Q, Xin S, Sun H, et al. Rapid-Charging Navigation of Electric Vehicles Based on Real-Time Power Systems and Traffic Data. IEEE Transactions on Smart Grid, 2014, 5(4):1969-1979.

[19] B. M. Davis and T. H. Bradley, The efficacy of electric vehicle time-of-use rates in guiding plug-in hybrid electric vehicle charging behavior, IEEE Trans. Smart Grid, 2012, 3(4):1679-1686.

[20] Tang D, Wang P. Nodal Impact Assessment and Alleviation of Moving Electric Vehicle Loads: From Traffic Flow to Power Flow. IEEE Trans. Power Syst, 2016, 31(6): 4231-4242.

[21] Motoaki Y, Shirk M G. Consumer behavioral adaption in EV fast charging through pricing. Energy Policy, 2017, 108.

[22] Hu Z, Zhan K, Zhang H, et al. Pricing mechanisms design for guiding electric vehicle charging to fill load valley. Applied Energy, 2016, 178:155-163.

[23] Islam S.Bayram, Michailidis G, Devetsikiotis M. Unsplittable load balancing in a network of charging stations under QoS guarantee. IEEE Trans. on Smart Grid, 2014, 6(3): 1292-1302.

[24] Dallinger D, Wietschel M. Grid integration of intermittent renewable energy sources using price-responsive plug-in electric vehicles. Renewable & Sustainable Energy Reviews, 2012, 16(5):3370-3382.

[25] Alizadeh M, Wai H T, Chowdhury M, et al. Optimal Pricing to Manage Electric Vehicles in Coupled Power and Transportation Networks. IEEE Transactions on Control of Network Systems, 2017, 4(4):863-875.

[26] He F, Yin Y, Wang J, et al. Sustainability SI: Optimal Prices of Electricity at Public Charging Stations for Plug-in Electric Vehicles. Networks & Spatial Economics, 2016, 16(1):131-154.

[27] National Development and Reform Commission of the People’s Republic of China, “Electric Vehicle Charging Infrastructure Development Guide”, Beijing, China, Oct. 9, 2015. [Online]. Available: http://www.sdpc.gov.cn/zcfb/zcfbtz/201511/t20151117_758762.html.

[28] National Energy Administration, “Electric Vehicle Charging infrastructure Promotion Alliance Annual Report in China”, Beijing, China, Jun. 19, 2017. [Online]. Available: http://www.nea.gov.cn/2017-06/19/c_136376732.htm.

[29] Golob T F. A simultaneous model of household activity participation and trip chain generation, Transportation Research Part B Methodological, 2000, 34(5):355-376.

[30] J. A. Bondy and U. S. R. Murty, Graduate Texts in Mathematics: Graph Theory, vol. 244. New York, NY, USA: Springer, 2008, pp. 1-34.

[31] Bowman J L, Ben-Akiva M E. Activity-based disaggregate travel demand model system with activity schedules, Transportation Research Part A Policy & Practice, vol.35, no.1, pp. 1-28, 2001.

[32] Kitamura R, Chen C, Pendyala R M, et al, Micro-simulation of daily activity-travel patterns for travel demand forecasting, Transportation, vol.27, no.1, pp. 25-51, 2000.

[33] K. Qian, C. Zhou, M. Allan, and Y. Yuan, Modeling of load demand due to EV battery charging in distribution systems, IEEE Trans. Power Syst., 2009, 26(2):802-810.

[34] U.S. Department of Transportation, Federal Highway Administration: National household travel survey. 2009, Available at: http://nhts.ornl.gov.

[35] Mauri, G., Valsecchi. A, Fast charging stations for electric vehicle: the impact on the MV distribution grids of the MILAN metropolitan area, 2012 IEEE Int. Energy Conf. and Exhibition, Florence, Italy, pp. 9-12, September 2012.

[36] Akhavan-Rezai, E., Shaaban, M.F., El-Saadany, E.F., et al, Uncoordinated charging impacts of electric vehicles on electric distribution grids: normal and fast charging comparison, 2012 IEEE Power and Energy Society General Meeting, San Diego, pp. 22 – 26, July 2012, USA.

[37] T. M. Chan, More algorithms for all-pairs shortest paths in weighted graphs, SIAM J. Comput., 2010, 39(5):2075-2089.

[38] Ghasemi M, Ghavidel S, Ghanbarian M M, et al. Multi-objective optimal power flow considering the cost, emission, voltage deviation and power losses using multi-objective modified imperialist competitive algorithm. Energy, 2014, 78(78):276-289.

[39] China Passenger Car Association (CPCA), Auto market analysis report of Dec. 2016, Shanghai, China, Feb., 2017. [Online]. Available: http://www.cpca1.org/newslist.asp?types=csjd&id=7102&page=4.

[40] Tao S, Liao K, Xiao X, et al. Charging demand for electric vehicle based on stochastic analysis of trip chain, Iet Generation Transmission & Distribution, 2016, 10(11):2689-2698.

[41] Hangzhou Comprehensive Transportation Research Center. [Online]. Available: http://www.hzjtydzs.com/.

[42] K. Jiguang, W. Zhenlin, C. Danming, and F. Xu, Research on electric vehicle charging mode and charging stations construction, (in Chinese) Power Demand Side Manage, 2009, 11(5):64-66.

[43] Xiang Y, Liu J, Li R, et al. Economic planning of electric vehicle charging stations considering traffic constraints and load profile templates[J]. Applied Energy, 2016, 178:647-659.

[44] Qian K, Zhou C, Allan M, et al. Modeling of Load Demand Due to EV Battery Charging in Distribution Systems. IEEE Transactions on Power Systems, 2011, 26(2):802-810.

[45] China Passenger Car Association (CPCA), Auto market analysis report of Dec. 2016, Shanghai, China, Feb., 2017. [Online]. Available: http://www.cpca1.org/newslist.asp?types=csjd&id=7102&page=4.

[46] Hangzhou people's government office, Implementation measure to promote the implementation of new energy electric vehicle charging infrastructure, Jun. 5, 2016. [Online]. Available: http://www.hangzhou.gov.cn/art/2016/6/1/art_1176017_3793.html.

[47] D. Liu, T. Qi, K. Zhang, and Y. Guo, Beijing residents' travel time survey in small samples, J. Transp. Syst. Eng. Inf. Technol., vol. 9, no. 2, Apr. 2009, pp. 23-26.

[48] Etezadi-Amoli M, Choma K, Stefani J. Rapid-charge electric-vehicle stations. IEEE Transactions on Power Delivery, 2010, 25(3): 1883-1887.